

A peer-reviewed version of this preprint was published in PeerJ on 6 April 2017.

[View the peer-reviewed version](https://peerj.com/articles/3134) (peerj.com/articles/3134), which is the preferred citable publication unless you specifically need to cite this preprint.

Jungbluth SP, Glavina del Rio T, Tringe SG, Stepanauskas R, Rappé MS. 2017. Genomic comparisons of a bacterial lineage that inhabits both marine and terrestrial deep subsurface systems. PeerJ 5:e3134 <https://doi.org/10.7717/peerj.3134>

Genomic comparisons of a bacterial lineage that inhabits both marine and terrestrial deep subsurface systems

Sean P Jungbluth^{Corresp., 1, 2}, Tijana Glavina del Rio³, Susannah G Tringe³, Ramunas Stepanauskas⁴, Michael S Rappé^{Corresp., 5}

¹ Department of Oceanography, University of Hawaii at Manoa, Honolulu, HI, United States

² Center for Dark Energy Biosphere Investigations, University of Southern California, Los Angeles, CA, United States

³ DOE Joint Genome Institute, Walnut Creek, CA, United States

⁴ Single Cell Genomics Center, Bigelow Laboratory for Ocean Sciences, East Boothbay, ME, United States

⁵ Hawaii Institute of Marine Biology, University of Hawaii at Manoa, Kaneohe, HI, United States

Corresponding Authors: Sean P Jungbluth, Michael S Rappé
Email address: jungbluth.sean@gmail.com, rappe@hawaii.edu

It is generally accepted that diverse, poorly characterized microorganisms reside deep within Earth's crust. One such lineage of deep subsurface-dwelling Bacteria is an uncultivated member of the *Firmicutes* phylum that can dominate molecular surveys from both marine and continental rock fracture fluids, sometimes forming the sole member of a single-species microbiome. Here, we reconstructed a genome from basalt-hosted fluids of the deep seafloor along the eastern Juan de Fuca Ridge flank and used a phylogenomic analysis to show that, despite vast differences in geographic origin and habitat, it forms a monophyletic clade with the terrestrial deep subsurface genome of "*Candidatus Desulforudis audaxviator*" MP104C. While a limited number of differences were observed between the marine genome of "*Candidatus Desulfopertinax cowenii*" modA32 and its terrestrial relative that may be of potential adaptive importance, here it is revealed that the two are remarkably similar thermophiles possessing the genetic capacity for motility, sporulation, hydrogenotrophy, chemoorganotrophy, dissimilatory sulfate reduction, and the ability to fix inorganic carbon via the Wood-Ljungdahl pathway for chemoautotrophic growth. Our results provide insights into the genetic repertoire within marine and terrestrial members of a bacterial lineage that is widespread in the global deep subsurface biosphere, and provides a natural means to investigate adaptations specific to these two environments.

1 **Genomic comparisons of a bacterial lineage that inhabits both marine and terrestrial deep**
2 **subsurface systems**

3

4 Sean P. Jungbluth^{1,2,*}, Tijana Glavina del Rio³, Susannah G. Tringe³, Ramunas Stepanauskas⁴,
5 and Michael S. Rappé^{5*}

6

7 ¹Department of Oceanography, SOEST, University of Hawaii, Honolulu, HI

8 ²Center for Dark Energy Biosphere Investigations, University of Southern California, Los
9 Angeles, CA

10 ³DOE Joint Genome Institute, Walnut Creek, CA

11 ⁴Single Cell Genomics Center, Bigelow Laboratory for Ocean Sciences, East Boothbay, ME

12 ⁵Hawaii Institute of Marine Biology, SOEST, University of Hawaii, Kaneohe, HI

13

14 *Corresponding authors: jungbluth.sean@gmail.com or rappe@hawaii.edu

15

16 Running title: Deep subsurface Firmicutes

17

18 KEY WORDS: deep subsurface · microorganisms · Firmicutes · Juan de Fuca Ridge ·
19 chemoautotrophy · basement biosphere · sulfate reduction · sporulation

20

21

22 **Abstract**

23 It is generally accepted that diverse, poorly characterized microorganisms reside deep within
24 Earth's crust. One such lineage of deep subsurface-dwelling Bacteria is an uncultivated member
25 of the *Firmicutes* phylum that can dominate molecular surveys from both marine and continental
26 rock fracture fluids, sometimes forming the sole member of a single-species microbiome. Here,
27 we reconstructed a genome from basalt-hosted fluids of the deep seafloor along the eastern
28 Juan de Fuca Ridge flank and used a phylogenomic analysis to show that, despite vast
29 differences in geographic origin and habitat, it forms a monophyletic clade with the terrestrial
30 deep subsurface genome of "*Candidatus Desulforudis audaxviator*" MP104C. While a limited
31 number of differences were observed between the marine genome of "*Candidatus*
32 *Desulfopertinax cowenii*" modA32 and its terrestrial relative that may be of potential adaptive
33 importance, here it is revealed that the two are remarkably similar thermophiles possessing the
34 genetic capacity for motility, sporulation, hydrogenotrophy, chemoorganotrophy, dissimilatory
35 sulfate reduction, and the ability to fix inorganic carbon via the Wood-Ljungdahl pathway for
36 chemoautotrophic growth. Our results provide insights into the genetic repertoire within marine
37 and terrestrial members of a bacterial lineage that is widespread in the global deep subsurface
38 biosphere, and provides a natural means to investigate adaptations specific to these two
39 environments.

40

41

42 Introduction

43 Recent progress in understanding the nature of microbial life inhabiting the sediment-
44 buried oceanic crust has been made through the use of ocean drilling program borehole
45 observatories as platforms to successfully sample fluids that percolate through the subseafloor
46 basement (Wheat et al., 2011). In 2003, a pioneering study by Cowen and colleagues used a
47 passive-flow device to collect microbial biomass from fluids emanating out of an over-pressured
48 borehole that originated from deep with the igneous basement of the eastern flank of the Juan de
49 Fuca Ridge in the Northeast Pacific Ocean (Cowen et al., 2003). Ribosomal RNA (rRNA) gene
50 cloning and sequencing from the crustal fluids led to the first confirmation of microbial life in
51 the deep marine igneous basement and revealed the presence of diverse Bacteria and Archaea.
52 Discovered in this initial survey was an abundant, uniquely branching lineage within the
53 bacterial phylum *Firmicutes* that was only distantly related to its closest known relative at the
54 time, a thermophilic nitrate-reducing chemoautotroph isolated from a terrestrial volcanic hot
55 spring, *Ammonifex degensii* (Huber et al., 1996).

56 Subsequent molecular surveys within both the terrestrial and marine deep subsurface
57 revealed the presence of microorganisms related to the original marine firmicutes lineage (Lin et
58 al., 2006; Jungbluth et al., 2013). In the deep subseafloor basement, this lineage has been
59 recovered in high abundance (up to nearly 40%) from basaltic crustal fluids collected from a
60 borehole nearby the initial location sampled ten years previously by Cowen and colleagues, as
61 well as from multiple boreholes spaced up to ~70 km apart in the same region of the Northeast
62 Pacific Ocean seafloor (Jungbluth et al., 2013; Jungbluth et al., 2014). In a surprising discovery,
63 a single ecotype closely related to this firmicutes lineage was discovered in deep terrestrial
64 subsurface fracture water of South Africa and found to be widespread (Magnabosco et al., 2014),

65 where it sometimes made up an extremely high proportion of microorganisms *in situ* (Chivian et
66 al., 2008). This lineage has since been found in other terrestrial habitats such as the
67 Fennoscandian Shield in Finland (Itävaara et al., 2011), a saline geothermal aquifer in Germany
68 (Lerm et al., 2013), and an alkaline aquifer in Portugal (Tiago & Veríssimo, 2013). Based on
69 ribosomal RNA sequence analyses, most of the terrestrial and marine lineages form a
70 monophyletic clade of predominantly subsurface origin but do not partition into subclades of
71 exclusively terrestrial and marine origin, suggesting that there may have been multiple
72 transitions between the terrestrial and marine deep subsurface environments (Jungbluth et al.,
73 2013).

74 In 2008, Chivian and colleagues reconstructed the first complete genome from a
75 terrestrial member of this firmicutes lineage, provisionally named “*Candidatus Desulforudis*
76 *audaxviator*” MP104C, via metagenome sequencing of a very low diversity sample from a deep
77 gold mine in South Africa (Chivian et al., 2008). The “*Ca. D. audaxviator*” genome revealed a
78 motile, sporulating, thermophilic chemolithoautotroph genetically capable of dissimilatory
79 sulfate reduction, hydrogenotrophy, nitrogen fixation, and carbon fixation via the reductive
80 acetyl-coenzyme A (Wood-Ljungdahl) pathway (Chivian et al., 2008). Thus, “*Ca. D.*
81 *audaxviator*” appears well suited for an independent lifestyle within the deep continental
82 subsurface environment. “*Ca. D. audaxviator*” and close relatives have continued to be recovered
83 in subsequent metagenomes sequenced from the South African subsurface (Lau et al., 2014).
84 Recently, five flow-sorted and single amplified genomes related to “*Ca. D. audaxviator*” were
85 sequenced from the terrestrial subsurface of South Africa, revealing significant genotypic
86 variation with the terrestrial genomes and providing evidence for horizontal gene transfer and
87 viral infection in the terrestrial subsurface environment (Labonté et al., 2015). To date,

88 knowledge regarding marine members of this deep subsurface firmicutes lineage has been
89 limited to phylogenetic (rRNA) and functional (dsr) gene surveys (Jungbluth et al., 2013;
90 Robador et al., 2015).

91 In this study, we sought to improve understanding of the functional and evolutionary
92 attributes of microorganisms inhabiting the deep seafloor basement by sequencing the
93 environmental DNA from two basement fluid samples from Juan de Fuca Ridge flank boreholes
94 U1362A and U1362B, generating the first metagenomes from this environment. Binning of the
95 resulting sequence data led to the reconstruction of a nearly complete genome closely related to
96 “*Ca. D. audaxviator*”. This genome has allowed us to compare the functional composition of
97 members of a microbial lineage that spans the terrestrial and marine deep subsurface, investigate
98 its evolutionary history, and determine its prevalence within a globally-distributed assemblage of
99 metagenomes.

100

101 **Materials and Methods**

102 *Borehole fluid sampling*

103 The methods used to collect samples during R/V Atlantis cruise ATL18_07 (28 June
104 2011 – 14 July 2011) are described elsewhere (Jungbluth et al., 2016). Briefly, basement crustal
105 fluids were collected from CORK observatories located in 3.5 million-year-old ocean crust east
106 of the Juan de Fuca spreading center in the Northeast Pacific Ocean. Basement fluids were
107 collected from the polytetrafluoroethylene (PTFE) lined fluid delivery lines associated with the
108 lateral CORKs (L-CORKs) at boreholes U1362A (47°45.6628’N, 127°45.6720’W) and U1362B
109 (47°45.4997’N, 127°45.7312’W). These lines extend to 200 and 30 meters below the sediment-
110 basement interface, respectively. Fluids were filtered *in situ* via a mobile pumping system

111 (Cowen et al., 2012) through Steripak-GP20 filter cartridges (Millipore, Billerica, MA, USA)
112 containing 0.22 μm pore-sized polyethersulfone membranes. A filtration rate of 1 liter min^{-1} was
113 calculated from laboratory tests, indicating that ~ 124 liters (U1362A) and ~ 70 liters (U1362B) of
114 deep subsurface crustal fluids were filtered.

115

116 *Metagenomic DNA sequencing*

117 Borehole fluid nucleic acids were extracted using a modified phenol/chloroform lysis and
118 purification method and is described in detail elsewhere (Jungbluth et al., 2016) (samples SSF21-
119 22 and SSF23-24). Library preparation and sequencing was conducted by the Joint Genome
120 Institute as part of the Community Sequencing Program. A total of 100 ng (U1362A) or 5 ng
121 (U1362B) of DNA was sheared using a focused-ultrasonicator (Covaris, Woburn, MA, USA).
122 The sheared DNA fragments were size selected using SPRI beads (Beckman Coulter, Brea, CA,
123 USA). The selected fragments from U1362A were then end-repaired, A-tailed, and ligated of
124 Illumina compatible adapters (Integrated DNA Technologies, Coralville, IA, USA) using KAPA-
125 Illumina library creation kit (KAPA Biosystems, Wilmington, MA, USA). The selected
126 fragments from U1362B were treated with end repair, ligation of adapters and 9 cycle of PCR on
127 the Mondrian SP+ Workstations (Nugen, San Carlos, CA, USA) using the Ovation SP+ Ultralow
128 DR Multiplex System kit (Nugen).

129 The library was quantified using KAPA Biosystem's next-generation sequencing library
130 qPCR kit and run on a LightCycler 480 real-time PCR instrument (Roche, Basel, Switzerland).
131 The quantified U1362A library was then prepared for sequencing on the HiSeq sequencing
132 platform (Illumina, San Diego, CA, USA) utilizing a TruSeq paired-end cluster kit, v3, and
133 Illumina's cBot instrument to generate clustered flowcell for sequencing. The U1362B library

134 was prepared for sequencing in the same manner except the library was multiplexed with another
135 sample library for a pool of 2 prior to use of the TruSeq kit. Sequencing of the flowcell was
136 performed on the Illumina HiSeq2000 sequencer using a TruSeq SBS sequencing kit 200 cycles,
137 v3, following a 2x150 indexed run recipe.

138 Insert size analysis was performed at JGI using bbmerge to pair overlapping reads and,
139 with sufficient coverage, non-overlapping reads using gapped kmers. The “percentage reads
140 joined” was calculated by (number of joined reads/total number of reads × 100). Raw reads were
141 used for the insert size calculation (no trimming or filtering). Insert size statistics for the U1362A
142 metagenome were: 68.342% reads joined, 216.60 bp average read length, 37.40 bp standard
143 deviation read length, and 215.00 bp mode read length. Insert size statistics for the U1362B
144 metagenome were: 50.40% reads joined, 210.80 bp average read length, 39.70 bp standard
145 deviation read length, and 196.00 mode read length.

146

147 *Metagenome quality control, read trimming and assembly*

148 Assembly was performed by the JGI; corresponding JGI assembly identifications are
149 1020465 (U1362A) and 1020462 (U1362B). Raw Illumina metagenomic reads were screened
150 against Illumina artifacts with a sliding window with a kmer size of 28, step size of 1. Screened
151 read portions were trimmed from both ends using a minimum quality cutoff of 3, reads with 3 or
152 more ‘Ns’ or with average quality score of less than Q20 were removed. In addition, reads with a
153 minimum sequence length of <50 bp were removed. Trimmed, screened, paired-end Illumina
154 reads were assembled using SOAPdenovo v1.05 (Luo et al., 2012) with default settings (options:
155 -K 81, -p 32, -R, -d 1) and a range of Kmers (81, 85, 89, 93, 97, 101). Contigs generated by each
156 assembly (six contig sets in total) were de-replicated using JGI in-house perl scripts. Contigs

157 were then sorted into two pools based on length. Contigs smaller than 1800 bp were assembled
158 using Newbler (Life Technologies, Carlsbad, CA, USA) in an attempt to generate larger contigs
159 (flags: -tr, -rip, -mi 98, -ml 80). All assembled contigs larger than 1800 bp were combined with
160 the contigs generated from the final Newbler run using minimus2 (flags: -D MINID=98 -D
161 OVERLAP=80) (Treangen et al., 2011). JGI-reported read depths available in IMG were
162 estimated based on read mapping with JGI in-house mapping programs.

163

164 *Gene prediction and annotation*

165 All aspects of metagenome annotation performed at JGI can be found at
166 img.jgi.doe.gov/m/doc/MetagenomeAnnotationSOP.pdf (Huntemann et al., 2016). Briefly,
167 metagenome sequences were preprocessed to resolve ambiguities, trim low-quality regions and
168 trailing 'N's using LUCY (Chou & Holmes, 2001), masked for low-complexity regions using
169 DUST (Morgulis et al., 2006), and dereplicated (95% threshold). Genes were predicted in the
170 following order: CRISPRs, non-coding RNA genes, protein-coding genes. CRISPR elements
171 were identified by concatenating the results from the programs CRT (Bland et al., 2007) and
172 PILER-CR (Edgar, 2007). tRNAs were predicted using tRNA scan SE-1.23 (Lowe & Eddy,
173 1997) three times using each of the domains of life (Bacteria, Archaea, Eukaryota) as the
174 parameter required; the best scoring predictions were selected. Fragmented tRNAs were
175 identified by comparison to a database of tRNAs identified in isolate genomes. Ribosomal RNA
176 genes were predicted using JGI-developed rRNA models (SPARTAN: SPecific & Accurate
177 rRNA and tRNA ANnotation). Protein-coding genes were identified using a majority rule-based
178 decision schema using four different gene callings tools: prokaryotic GeneMark (hmm version
179 2.8) (Lukashin & Borodovsky, 1998) Metagene Annotator v1.0 (Noguchi, Park & Takagi, 2006),

180 Prodigal v2.5 (Hyatt et al., 2012) and FragGeneScan v1.16 (Rho, Tang & Ye, 2010). When there
181 was no clear decision, the selection was based on preference order of gene callers determined by
182 JGI-based runs on simulated metagenomic datasets [GeneMark > Prodigal > Metagenome >
183 FragGeneScan].

184 Predicted CDSs were translated and associated with Pfams COGs, KO terms, EC
185 numbers, and phylogeny. Genes were associated with Pfam-A using hmmsearch (Durbin et al.,
186 1998). Genes were associated with COGs by comparing protein sequences with the database of
187 PSSMs for COGs downloaded from NCBI; rpsblast v2.26 (Marchler-Bauer et al., 2003) was
188 used to find hits. Assignments of KO terms, EC numbers, and phylogeny were made using
189 similarity searches to reference databases constructed by starting with the set of all non-
190 redundant sequences taken from public genomes in IMG. Sequences from the KEGG database
191 that were not present in IMG were added and all data was merged to related gene IDs to taxa,
192 KO terms, and EC numbers. USEARCH (Edgar, 2010) was used to compare predicted protein-
193 coding genes to genes in this database and the top five hits for each gene were retained.
194 Phylogenetic assignment was based on the top hit only; for assignment of KO terms, the top 5
195 hits to genes in the KO index were used. A hit resulted in an assignment if there was at least 30%
196 identity and greater than 70% of the query protein sequence or the KO gene sequence were
197 covered by the alignment.

198

199 *Genomic bin identification and reconstruction*

200 All metagenomic scaffolds greater than 200 basepairs (bp) from U1362A (n=137,672
201 contigs) and U1362B (n=212,542 contigs) were binned separately with MaxBin v1.4 (Wu et al.,
202 2014) using the 40 marker gene set universal among bacteria and archaea (Wu, Jospin & Eisen,

203 2013), minimum contig length of 1000 bp, and default parameters. Contig coverage from each
204 metagenome was estimated using the quality control-filtered raw reads as input for mapping
205 using Bowtie2 v2.1.0 (Langmead & Salzberg 2012) via MaxBin. The genomic bins were
206 screened and analyzed for completeness, contamination, and assigned taxonomic identifications
207 using CheckM v1.0.5 (Parks et al., 2015) with default parameters.

208 Raw quality control-filtered sequence reads from the U1362A and U1362B metagenomes
209 related to “*Ca. D. audaxviator*” were identified by mapping to three sources: (1) a single
210 genomic bin from U1362A related to “*Ca. D. audaxviator*” identified via CheckM (bin A32), (2)
211 the “*Ca. D. audaxviator*” genome, (3) and all “*Ca. D. audaxviator*”-related contigs > 200 bp from
212 the U1362A and U1362B metagenome assemblies generated by the Joint Genome Institute.
213 Mapping was performed independently for the U1362A and U1362B metagenomes using both
214 the bbmap v34.25 (<http://sourceforge.net/projects/bbmap/>) and Bowtie2 v2.1.0 (Langmead &
215 Salzberg 2012) software packages with default parameters and the paired-end read-mapping
216 feature (Supplementary Table 1). All reads from the U1362A metagenome mapping to any of the
217 three sources (1,785,284 sequences) were assembled using SPAdes v3.5.0 (Bankevich et al.,
218 2012) with options `-k: 21,33,55,77, --careful -pe1-12` and default parameters. Contaminating
219 contigs in the assembly were screened and removed using the JGI ProDeGe web portal v2.0
220 (<https://prodege.jgi-psf.org/>) on April 10, 2015, using default parameters with the following
221 taxonomy specified: “Bacteria; Firmicutes; Clostridia” (Tenessen et al., 2016). Contigs
222 remaining following the use of ProDeGe comprise the genome bin henceforth named “*Ca.*
223 *Desulfofopertinax cowenii*” modA32 and were screened using CheckM as described above.

224

225 *Genome annotation and analysis*

226 The modified genome bin resulting from the pipeline described above (“*Ca. D. cowenii*”
227 modA32) was annotated via the Joint Genome Institute’s Integrated Microbial Genomes-Expert
228 Review (IMG-ER) web portal (Markowitz et al., 2014; Huntemann et al., 2015). Annotations in
229 the IMG-ER web portal served as the source of reported genome characteristics and reported
230 genes and their assignment to COGs. Phylogenetically informative marker genes from “*Ca. D.*
231 *cowenii*” were identified and extracted using the ‘tree’ command in CheckM. In CheckM, open
232 reading frames were called using prodigal v2.6.1 (Hyatt et al., 2012) and a set of 43 lineage-
233 specific marker genes, similar to the universal set used by PhyloSift (Darling et al., 2014), were
234 identified and aligned using HMMER v3.1b1 (Eddy, 2011). Initial phylogenetic analysis used
235 pplacer (v1.1.alpha16-1-gf748c91) (Matsen, Kodner & Armbrust, 2010) to place sequences into
236 a CheckM tree/database (version 0.9.7) composed of 2052 finished and 3604 draft genomes
237 (Markowitz et al., 2012).

238 An alignment 6988 amino acids in length corresponding to the 43 concatenated marker
239 genes from “*Ca. D. cowenii*”, “*Ca. D. audaxviator*”, other *Firmicutes*, and *Actinobacteria* were
240 used for additional phylogenetic analysis. The concatenated amino acid alignment was used to
241 generate a phylogeny using FastTree v2.1.9 (Price, Dehal & Arkin, 2010) with the WAG amino
242 acid substitution model. The dendrogram was visualized using iTOL v3 (Letunic and Bork,
243 2016).

244 Average nucleotide identity (ANI) was computed in IMG-ER using pairwise bidirectional
245 best nSimScan hits of genes having 70% or more identity and at least 70% coverage of the
246 shorter gene. The “*Ca. D. cowenii*” → [other genome] values are reported. Protein-coding genes
247 in “*Ca. D. cowenii*” with and without homologs in “*Ca. D. audaxviator*”, and vice versa, were
248 identified and percent similarity estimated using the “Phylogenetic Profiler” tool in IMG-ER

249 with default parameters (max e-value: $10e^{-5}$; minimum identity: 30%). Average amino acid
250 identity (AAI) was computed for pairs of genomes closely related to “*Ca. D. cowenii*” with an
251 online web tool (<http://enve-omics.ce.gatech.edu/aai/>) using default parameters. All non-RNA
252 genes at least 100 amino acids in length were used in this analysis. Two-way average amino acid
253 identity scores are reported and the percent shared genes were calculated as follows: $100 \times (2 \times$
254 $[\text{number of proteins used for two-way AAI analysis}] / ([\text{total number of amino acids} \geq 100 \text{ from}$
255 $\text{genome A}] + [\text{total number of amino acids} \geq 100 \text{ from genome B}])$. Estimates of transposase and
256 integrase abundance were derived in IMG using a functional profile of 100 pfams and COG
257 functions selected searching for keywords “transposase” and “integrase”.

258

259 *Genome and scaffold visualizations*

260 Global genome comparisons were visualized in Circos v0.67-5 (Krzywinski et al., 2009).
261 Links between genomic regions of “*Ca. D. cowenii*” and “*Ca. D. audaxviator*” represent best
262 reciprocal BLAST hits, which were generated using the `blast_rbh.py` script
263 (https://github.com/peterjc/galaxy_blast/tree/master/tools/blast_rbh) with `blastn v2.2.29`
264 (Altschul et al., 1990) and default parameters. Links between genomic regions from the single
265 amplified genomes of Labonté et al. (Labonté et al., 2015) represent BLAST hits that were
266 generated using `blastn` with default parameters and using “*Ca. D. cowenii*” and “*Ca. D.*
267 *audaxviator*” as reference databases.

268 Selected scaffold regions were visualized with Easyfig v2.2.2 (Sullivan, Petty & Beatson,
269 2011). Similarity between regions was assessed using BLAST wrapped within Easyfig using
270 default parameters and task: `blastn`; minimum hit length: 50; max e-value: 0.001; minimum
271 identity value: 50. In all instances of blast, contigs from “*Ca. D. cowenii*” were used as the query

272 and “*Ca. D. audaxviator*” was used as the reference, with the exception of the single three-
273 scaffold comparison where “*Ca. D. audaxviator*” was used as the query and “*Ca. D. cowenii*”
274 Ga007115_16 used as the reference.

275

276 *Metagenome fragment recruitment*

277 Quality-filtered raw reads from the U1362A and U1362B metagenomes were mapped to
278 the six scaffolds that make up the “*Ca. D. cowenii*” genome bin and the “*Ca. D. audaxviator*”
279 genome. Recruitment was performed using FR-HIT v0.7.1 (Niu et al., 2011) with default
280 parameters (minimum sequence similarity 75%) and reporting a single best top hit for each read
281 (-r 1).

282

283 *Analysis of metagenome-derived SSU rRNA genes*

284 Full length SSU rRNA genes from the raw quality-filtered U1362A metagenome reads
285 were assembled using EMIRGE (Miller et al., 2011) with default parameters and -a 20, -i 270, -s
286 100, -l 150, -j 1.0, --phred33, and using the SILVA SSURef_Nr99 version 119 database that was
287 prepared using the fix_nonstandard_chars.py script supplied on the EMIRGE website
288 (<https://github.com/csmiller/EMIRGE>). Out of 1951 near full-length SSU rRNA sequences
289 constructed after 67 iterations of EMIRGE, a single sequence related to the “*Ca. D. audaxviator*”
290 lineage was identified through the SILVA online portal (Pruesse, Peplies & Glöckner, 2012).
291 The sequence was aligned using the SINA online aligner and manually curated in ARB (Ludwig
292 et al., 2004). Ambiguous and mis-aligned positions were excluded from further analysis.

293 A base SSU rRNA gene phylogenetic tree was reconstructed in ARB from 36 sequences
294 and an alignment of 797 nucleotide positions using RAxML v7.72 (Stamatakis, 2006) with

295 default parameters, the GTR+G+I nucleotide substitution model identified via JModelTest v2.1.1
296 (Darriba et al., 2012), and selecting the best tree from 100 iterations. Bootstrapping was
297 performed in ARB using the RAxML tool with 2000 replicates (Stamatakis, Hoover &
298 Rougemont, 2008). Sequences of short length, including a masked version of the “*Ca. D.*
299 *audaxviator*” -related SSU rRNA gene found here, were added to the phylogeny using the
300 parsimony insertion tool in ARB and a filter containing 363 nucleotide positions.

301

302 *Phylogenetic analysis of dsrAB gene sequences*

303 DNA sequences corresponding to dissimilatory sulfite reductase subunits alpha and beta
304 (*dsrAB*) were aligned in ARB using the ‘integrated aligners’ tool and a previously published
305 database of aligned *dsrAB* sequences (Loy et al., 2009). Additional sequences were identified
306 and included via BLAST search of the non-redundant NCBI database using megablast and blastn
307 with default parameters. Phylogenetic analyses were performed individually for *dsrA* and *dsrB*
308 using RAxML with the GTR model of nucleotide substitution under the gamma- and invariable-
309 models of rate heterogeneity, identified via jModelTest. The tree with the highest negative log-
310 likelihood score was selected from performing 100 iterations using RAxML with default
311 parameters. Phylogenies for the base trees were derived from partial length *dsrA* and *dsrB*
312 alignments (545 and 303 nucleotides, respectively) and bootstrapping was performed in ARB
313 using the RAxML rapid bootstrap analysis algorithm with 2000 bootstraps.

314

315 *Analysis of global distribution patterns*

316 All protein-coding genes corresponding to the genomes of “*Ca. D. cowenii*” (1782 genes)
317 and “*Ca. D. audaxviator*” (2239 genes) were used to generate a profile against 489 globally-

318 distributed metagenomes from marine subsurface fluids, the terrestrial subsurface, terrestrial hot
319 springs, marine sediments, and seawater (Supplementary Table 2). In IMG-ER, the “Profile &
320 Alignment” tool was used to query assembled metagenomes using genes corresponding to the
321 two genomes, a maximum e-value of 10^{-5} , and a minimum similarity of 70%. The number of
322 gene hits was converted to a relative frequency and the location of hits was visualized in R
323 v3.1.2 (R Core Team, 2015) using latitude and longitude information provided as metadata and
324 the R maps package (version 2.3-10).

325 Fragment recruitment was subsequently used in effort to discriminate between the
326 distribution of the marine (“*Ca. D. cowenii*’ modA32A) and terrestrial (“*Ca. D. audaxviator*”)
327 genomes of this *Firmicutes* lineage. Raw reads corresponding to IMG-ER metagenomes with the
328 highest hit frequencies in the profiles generated in IMG, and additional unamplified
329 metagenomes from the marine and terrestrial subsurface available only via NCBI sequence read
330 archive and MG-RAST, were used as references for mapping to the genomes of “*Ca. D.*
331 *cowenii*” and “*Ca. D. audaxviator*” (Supplementary Table 3). In order to determine a %
332 similarity cutoff that can discriminate between the two targets, the two genomes were cut into
333 non-overlapping 150 bp fragments to simulate the most common sequence read length in current
334 metagenome projects, and mapped back to the intact “*Ca. D. cowenii*” and “*Ca. D. audaxviator*”
335 genomes using FR-HIT with default parameters, restricting matches to the single top best hit.
336 Percent similarities ranging from 70-100% were tested in one percent increments in order to
337 quantify the frequency that the fragmented genomes map to their source genome. A 96%
338 similarity level was ultimately used because it restricted spurious matches (i.e. reads mapping
339 from one genome to the other) to a frequency of ~1% (Supplementary Figure 1). The ratio of

340 reads mapping to “*Ca. D. cowenii*” or “*Ca. D. audaxviator*” was calculated and visualized using
341 Circos.

342

343 *Sample access and affiliated information*

344 The annotated draft genome of “*Ca. D. cowenii*” modA32 is available via the IMG web
345 portal under Taxon ID number 2615840622 (Gold Analysis Project ID: Ga0071115). The
346 U1362A and U1362B metagenomes are available via the IMG-M web portal under Taxon ID
347 numbers 330002481 and 3300002532, respectively. Gold Analysis Project ID numbers are
348 Ga0004278 (U1362A) and Ga0004277 (U1362B). Sample metadata can be accessed using the
349 BioProject identifier PRJNA269163. The NCBI BioSamples used here are SAMN03166137
350 (U1362A) and SAMN03166138 (U1362B). Raw sequence data can be accessed using NCBI
351 SRA identifiers SRR3723048 (U1362A) and SRR3732688 (U1362B).

352

353 **Results and Discussion**

354 *Bin identification and refinement*

355 Of 60 and 41 genome bins representing diverse groups of uncultivated bacteria and
356 archaea reconstructed from the U1362A and U1362B metagenomes, respectively, one that
357 comprised a nearly complete genome from U1362A (bin A32) was preliminarily identified as
358 related to “*Ca. D. audaxviator*” by phylogenetic analyses of a set of concatenated single copy
359 marker genes. In order to maximize genome recovery while minimizing potential contamination,
360 contigs within genome bin A32, the “*Ca. D. audaxviator*” genome, and scaffolds related to “*Ca.*
361 *D. audaxviator*” that were assembled directly from the U1362A and U1362B metagenomes were
362 used as references for mapping raw sequence reads from the U1362A and U1362B metagenomes

363 via several read mapping methods. Sequence mate pairs from the U1362A metagenome that
364 mapped to these templates were pooled and reassembled (Supplementary Table 1). Following
365 subsequent screening and removal of contaminating sequences (Supplementary Table 4), six
366 genomic scaffolds totaling 1,778,734 base pairs (bp) in length were identified that correspond to
367 the draft “*Ca. D. cowenii*” modA32 genome described here (Table 1). The purity of the modified
368 genomic bin was supported by results generated using CheckM (Parks et al., 2015) (Table 2),
369 congruent phylogenetic analyses of concatenated marker genes (Figure 1A) and *dsrB* (Figure
370 2A) and *dsrA* genes (Supplementary Figure 2), and a high percent of shared genes and gene
371 synteny between the six genomic scaffolds of “*Ca. D. cowenii*” and the “*Ca. D. audaxviator*”
372 genome (Figures 1B and 3A).

373 The 1.78 Mbp “*Ca. D. cowenii*” modA32 genome is 98-99% complete based on separate
374 analyses of tRNA and other marker gene content specific to the phylum *Firmicutes* (Table 1). A
375 phylogenomic analysis of 43 conserved marker genes confirmed a monophyletic relationship
376 between “*Ca. D. cowenii*” and “*Ca. D. audaxviator*” within the *Firmicutes* (Figure 1A), a
377 relationship that was also supported by analyses of both *dsrA* (Supplementary Figure 2) and *dsrB*
378 genes (Figure 2A). While no small-subunit (SSU) rRNA genes were identified in the “*Ca. D.*
379 *cowenii*” genome bin, a single full-length SSU rRNA gene related to “*Ca. D. audaxviator*” was
380 reconstructed from raw U1362A metagenome reads. Phylogenetic analyses revealed this gene to
381 form a tight cluster with SSU rRNA genes recovered previously from the deep seafloor along
382 the Juan de Fuca Ridge flank and, more broadly, a monophyletic lineage with “*Ca. D.*
383 *audaxviator*” within the phylum *Firmicutes* (Figure 2B). Consistent with previous studies
384 (Jungbluth et al., 2014; Jungbluth et al., 2016), oceanic crustal fluid SSU rRNA gene clones
385 formed at least two independent sub-lineages within this clade (Figure 2B).

386

387 *Comparative genomics*

388 The genomes of “*Ca. D. cowenii*” and “*Ca. D. audaxviator*” share an average nucleotide
389 identity of 76.9%, which is almost 7% higher than “*Ca. D. cowenii*” shares with the next most
390 similar firmicutes genome, *Desulfovirgula thermocuniculi*. Similarly, the genomes of “*Ca. D.*
391 *cowenii*” and “*Ca. D. audaxviator*” share an average amino acid identity of 74.2%, a value that is
392 almost 18% higher than “*Ca. D. cowenii*” shares with its next most similar genome, the firmicute
393 *Desulfotomaculum kuznetsovii* DSM 6115 (Figure 1B). A similar result was obtained by
394 quantifying the proportion of genes shared between “*Ca. D. cowenii*” and “*Ca. D. audaxviator*”
395 (73.2%) (Figure 1B).

396 Compared to the genomes of its closest relatives, the 1.78 Mbp genome harbored by “*Ca.*
397 *D. cowenii*” is small (Figure 1B). Despite the smaller size of the “*Ca. D. cowenii*” genome
398 compared to the 2.35 Mbp genome of “*Ca. D. audaxviator*”, the two share similar coding density
399 (89.8% vs. 87.6%), resulting in 451 fewer genes in “*Ca. D. cowenii*” (1842 vs. 2293) (Table 1).
400 Compared to other firmicutes, the predicted genome size of “*Ca. D. cowenii*” is among the
401 smallest for members of the Class *Clostridia* with an elevated %GC (Figure 4). The smaller
402 genome of “*Ca. D. cowenii*” shares 1514 of its 1782 (85.0%) protein coding genes with “*Ca. D.*
403 *audaxviator*”. Despite the lower gene content overall, “*Ca. D. cowenii*” harbors a similar number
404 of protein coding genes with a predicted function as the genome of “*Ca. D. audaxviator*” (1518
405 vs. 1587) (Table 1). In addition to a smaller genome and fewer genes, “*Ca. D. cowenii*” also
406 contained fewer pseudogenes (0 vs. 82) and paralogs (137 vs. 265) in comparison to “*Ca. D.*
407 *audaxviator*” (Table 1), which together suggest some form of streamlining of the “*Ca. D.*
408 *cowenii*” genome. Compared to “*Ca. D. audaxviator*”, the genome of “*Ca. D. cowenii*” contains

409 fewer CRISPR elements, integrases and transposases, and phage-related genes, which suggests
410 lower viral infection and less horizontal gene transfer in the marine lineage.

411 Extensive gene synteny between “*Ca. D. cowenii*” and “*Ca. D. audaxviator*” was
412 revealed by comparing locations of homologs (Figures 3A and 3B). Aligning the genome of “*Ca.*
413 *D. cowenii*” with five incomplete (3.6-7.8% complete) single amplified genomes (SAGs)
414 isolated from the terrestrial South Africa subsurface and related to “*Ca. D. audaxviator*”
415 (Labonté et al., 2015) revealed that all of the SAGs were more similar to “*Ca. D. audaxviator*”
416 than “*Ca. D. cowenii*” (Figure 5).

417

418 *Similarities in functional gene complement*

419 Comparisons of predicted proteins assigned to clusters of orthologous groups (COGs)
420 revealed a markedly similar distribution within the “*Ca. D. cowenii*” and “*Ca. D. audaxviator*”
421 genomes (Figure 3C). A detailed description of these shared features is included in
422 Supplementary Table 5.

423 The genome of “*Ca. D. cowenii*” reveals a microorganism that is functionally similar to
424 “*Ca. D. audaxviator*”: an independent lifestyle consisting of a motile, sporulating, thermophilic,
425 anaerobic chemolithoautotroph genetically capable of dissimilatory sulfate reduction,
426 hydrogenotrophy, carbon fixation via the reductive acetyl-coenzyme A (Wood-Ljungdahl)
427 pathway, and synthesis of all amino acids. The genome of “*Ca. D. cowenii*” also indicates a
428 chemoorganotroph that possesses abundant sugar transporters and is capable of glycolysis, which
429 is somewhat surprising given the low dissolved organic carbon concentrations in this system (Lin
430 et al., 2012). Similar to “*Ca. D. audaxviator*”, hydrogenases were abundant in “*Ca. D. cowenii*”,
431 which is consistent with the availability of hydrogen in basement fluids of the Juan de Fuca

432 Ridge flank (Lin et al., 2014). Altogether, the shared features between “*Ca. D. cowenii*” and
433 “*Ca. D. audaxviator*” help to explain the wide distribution of this lineage in the global deep
434 subsurface.

435

436 *Differences in functional gene complement*

437 Despite highly similar genomes overall, comparisons of predicted proteins assigned to
438 clusters of orthologous groups (COGs) revealed unique genes in “*Ca. D. cowenii*” that were not
439 found in “*Ca. D. audaxviator*” (Figure 3D; also see Supplementary Tables 6 and 7). These genes
440 are likely locations to uncover features that differentiate the marine versus terrestrial members of
441 this lineage. While most unique genes in the “*Ca. D. cowenii*” genome have general functional
442 characterizations only (COG category R), the largest fraction of unique genes in the “*Ca. D.*
443 *cowenii*” versus “*Ca. D. audaxviator*” genome are found within COG category M (Cell
444 wall/membrane/envelop biogenesis) and include nucleoside-diphosphate-sugar epimerases (e.g.
445 *galE*) and glycosyltransferases (e.g. *treT*) involved in cell wall biosynthesis, and possibly in the
446 production of exopolysaccharides involved with biofilm formation. Defense mechanisms (COG
447 category V) contained the highest ratio of unique genes in the “*Ca. D. cowenii*” genome
448 compared to “*Ca. D. audaxviator*” and includes genes related to ABC-type multidrug transport
449 systems, multidrug resistance efflux pumps (*hylD*), and a class-A beta-lactamase. The marine
450 genome has numerous monosaccharide transporters not present in the terrestrial genome,
451 including those encoding for components of ribose/xylose, arabinose, methyl-galactoside,
452 xylose, allose, and rhamnose transport. Thus, potential differences in organic carbon substrate
453 specificity are evident.

454 Though the genome of “*Ca. D. cowenii*” is incomplete, within assembled contigs there
455 are a small number of large indels that are also potential sources of functional differentiation
456 between “*Ca. D. cowenii*” and “*Ca. D. audaxviator*”. An indel present in “*Ca. D. audaxviator*”
457 but lacking in “*Ca. D. cowenii*” includes a nitrogenase operon as well as genes for ammonium
458 transport and nitrogen regulation (Figure 6). While the genes for glutamine synthetase and
459 glutamate synthase within the genome of “*Ca. D. cowenii*” suggest that it obtains its nitrogen
460 from the abundant ammonia in Juan de Fuca Ridge flank crustal fluids (Lin et al., 2012), it
461 appears to be unable to fix inorganic dinitrogen. Another indel suggests that “*Ca. D. cowenii*”
462 lacks the capacity to produce cobalamin (Figure 6). Moreover, a large cassette of genes present
463 in the “*Ca. D. audaxviator*” genome that is related to gas vesicle production (and flanked by an
464 integrase and two transposases) is missing in “*Ca. D. cowenii*”. Finally, CRISPR-CAS gene
465 arrays and CRISPR elements were distinct between the two genomes (Figure 6), with the
466 genome of “*Ca. D. cowenii*” encoding 14 CRISPR-associated proteins versus 25 in “*Ca. D.*
467 *audaxviator*”.

468

469 *Distribution*

470 The Desulfopertinax/Desulforudis lineage was detected in metagenomic data generated
471 from the terrestrial subsurface of Mt. Terri, Switzerland and the Coast Range Ophiolite,
472 California, USA (Figure 7A; see also Supplementary Table 2). It was also found within marine
473 sediments from the coastal Atlantic and Pacific, a Yellowstone National Park hot spring, and the
474 terrestrial subsurface in Ontario, Canada, but never identified in seawater worldwide. Mapping
475 raw metagenome reads in a lineage-specific manner that discriminated between reads mapping to
476 “*Ca. D. audaxviator*” and “*Ca. D. cowenii*” revealed partitioning of these genomes between

477 terrestrial and marine environments, respectively (Figure 7B; see also Supplementary Table 3).
478 Surprisingly, the ratio of mapped reads from “*Ca. D. cowenii*” to “*Ca. D. audaxviator*” was,
479 highest (18.9) in a sample from the terrestrial subsurface. The next largest ratios were from the
480 U1362A metagenome (7.3), three serpentinite groundwater metagenomes (1.7-1.6), and the
481 U1362B metagenome (1.4). The ratio of “*Ca. D. audaxviator*” to “*Ca. D. cowenii*” reads was
482 highest (up to ~165) in samples collected from the terrestrial subsurface of Witwatersrand Basin,
483 South Africa, although this lineage also appears present in serpentinite fluids from the terrestrial
484 subsurface. Thus, it appears that the *Desulfopertinax/Desulforudis* lineage has a cosmopolitan
485 distribution throughout the global subsurface environment, as indicated by mapping reads from
486 489 metagenomes from the terrestrial and marine subsurface to the genomes of “*Ca. D. cowenii*”
487 and “*Ca. D. audaxviator*”, as well as gene clones identified in published SSU rRNA surveys
488 (Figure 7; see also Figure 2B and Supplementary Tables 2 and 3).

489

490 **Conclusions**

491 Crustal fluids within the terrestrial and marine deep subsurface contain microbial life
492 living at the biosphere’s limit; globally, deep subsurface biosphere is thought be one of the
493 largest reservoirs for microbial life on our planet. This study takes advantage of new sampling
494 technologies and couples them with improvements to DNA sequencing and associated
495 informatics tools in order to reconstruct the genome of an uncultivated *Firmicutes* bacterium
496 from fluids collected deep within the seafloor of the Juan de Fuca Ridge flank that has
497 previously been documented within both the terrestrial and marine subsurface. Based on our
498 analyses, the capacity for both autotrophic and heterotrophic lifestyles combined with motility
499 and sporulation confers upon “*Ca. D. cowenii*” and “*Ca. D. audaxviator*” the ability to colonize

500 the global deep biosphere. We believe this to be the only microbial lineage known to inhabit both
501 marine and terrestrial deep subsurface systems, providing a unique opportunity to advance our
502 understanding of subsurface microbiology. By comparing the genome of this microorganism to a
503 terrestrial counterpart, we reveal a high and unsuspected degree of functional similarity spanning
504 the marine and terrestrial members of this lineage. Based on the predicted ability to reduce
505 sulfate for energy generation, the persistent detection of this lineage in deep marine biosphere
506 studies, and its initial discovery by deep seafloor pioneer James Cowen, we propose the name
507 “*Desulfopertinax cowenii*” for this candidatus taxon.

508

509 **Acknowledgements**

510 We thank the captain and crew, A. Fisher, K. Becker, C. G. Wheat, and other members of
511 the science teams on board R/V Atlantis cruise AT18-07. We thank Beth Orcutt for facilitating
512 metagenome sequencing. We also thank the pilots and crew of remote-operated vehicle *Jason II*.
513 We thank Brian Foster and Alex Copeland of the JGI for initial assembly of the metagenomes.
514 We thank Sean Cleveland and the Hawaii HPC facility. This research was supported by funding
515 from National Science Foundation grants MCB06-04014 and OCE-1260723 (to MSR) and OCE-
516 1136488 (to RS), the Center for Dark Energy Biosphere Investigations, a National Science
517 Foundation-funded Science and Technology Center of Excellence (NSF award OCE-0939564),
518 and from Department of Energy Joint Genome Institute Community Sequencing Award 987 (to
519 RS). The work conducted by the U.S. Department of Energy Joint Genome Institute, a DOE
520 Office of Science User Facility, is supported by the Office of Science of the U.S. Department of
521 Energy under Contract No. DE-AC02-05CH11231. This study used samples and data provided

522 by the Integrated Ocean Drilling Program. This is SOEST contribution XXXX, HIMB
523 contribution XXXX, and C-DEBI contribution XXXX.

524

525 **References**

- 526 Altschul SF, Gish W, Miller W, Myers EW, Lipman DJ. (1990). Basic local alignment search
527 tool. *J Mol Biol* 215:403–410. DOI: 10.1016/S0022-2836(05)80360-2.
- 528 Bankevich A, Nurk S, Antipov D, Gurevich AA, Dvorkin M, Kulikov AS, *et al.* (2012). SPAdes:
529 a new genome assembly algorithm and its applications to single-cell sequencing. *J*
530 *Comput Biol* 19:455–477. DOI: 10.1089/cmb.2012.0021.
- 531 Bland C, Ramsey TL, Sabree F, Lowe M, Brown K, Kyrpides NC, *et al.* (2007). CRISPR
532 recognition tool (CRT): a tool for automatic detection of clustered regularly interspaced
533 palindromic repeats. *BMC Bioinformatics* 8:209. DOI: 10.1186/1471-2105-8-209.
- 534 Chivian D, Brodie EL, Alm EJ, Culley DE, Dehal PS, DeSantis TZ, *et al.* (2008). Environmental
535 genomics reveals a single-species ecosystem deep within Earth. *Science* 322:275–278.
536 DOI: 10.1126/science.1155495.
- 537 Chou HH, Holmes MH. (2001). DNA sequence quality trimming and vector removal.
538 *Bioinformatics* 17:1093–1104. DOI: 10.1093/bioinformatics/17.12.1093.
- 539 Cowen JP, Copson DA, Jolly J, Hsieh C-C, Lin H-T, Glazer BT, *et al.* (2012). Advanced
540 instrument system for real-time and time-series microbial geochemical sampling of the
541 deep (basaltic) crustal biosphere. *Deep Sea Res Pt I* 61:43–56. DOI:
542 10.1016/j.dsr.2011.11.004.
- 543 Cowen JP, Giovannoni SJ, Kenig F, Johnson HP, Butterfield D, Rappé MS, *et al.* (2003). Fluids
544 from aging ocean crust that support microbial life. *Science* 299:120–123. DOI:
545 10.1126/science.1075653.
- 546 Darling AE, Jospin G, Lowe E, Matsen FA, Bik HM, Eisen JA. (2014). PhyloSift: phylogenetic
547 analysis of genomes and metagenomes. *PeerJ* 2:e243. DOI: 10.7717/peerj.243.
- 548 Darriba D, Taboada GL, Doallo R, Posada D. (2012). jModelTest 2: more models, new heuristics
549 and parallel computing. *Nat Methods* 9:772. DOI: 10.1038/nmeth.2109.
- 550 Durbin R, Eddy SR, Krogh A, Mitchison G. (1998). Biological sequence analysis: probabilistic
551 models of proteins and nucleic acids. Cambridge: Cambridge University Press.

- 552 Eddy SR. (2011). Accelerated Profile HMM Searches. *PLoS Comput Biol* 7:e1002195. DOI:
553 10.1371/journal.pcbi.1002195.
- 554 Edgar RC. (2007). PILER-CR: fast and accurate identification of CRISPR repeats. *BMC*
555 *Bioinformatics* 8:18. DOI: 10.1186/1471-2105-8-18.
- 556 Edgar RC. (2010). Search and clustering orders of magnitude faster than BLAST. *Bioinformatics*
557 26:2460–2461. DOI: 10.1093/bioinformatics/btq461.
- 558 Huber R, Rossnagel P, Woese CR, Rachel R, Langworthy TA, Stetter KO. (1996). Formation of
559 ammonium from nitrate during chemolithoautotrophic growth of the extremely
560 thermophilic bacterium *Ammonifex degensii* gen. nov. sp. nov. *Syst Appl Microbiol*
561 19:40–49. DOI: 10.1016/S0723-2020(96)80007-5.
- 562 Huntemann M, Ivanova NN, Mavromatis K, Tripp HJ, Paez-Espino D, Palaniappan K, *et al.*
563 (2015). The standard operating procedure of the DOE-JGI Microbial Genome Annotation
564 Pipeline (MGAP v.4). *Stand Genomic Sci* 10:86. DOI: 10.1186/s40793-015-0077-y.
- 565 Huntemann M, Ivanova NN, Mavromatis K, Tripp HJ, Paez-Espino D, Tennesen K, *et al.*
566 (2016). The standard operating procedure of the DOE-JGI Metagenome Annotation
567 Pipeline (MAP v.4). *Stand Genomic Sci* 11:17. DOI: 10.1186/s40793-016-0138-x.
- 568 Hyatt D, LoCascio PF, Hauser LJ, Uberbacher EC. (2012). Gene and translation initiation site
569 prediction in metagenomic sequences. *Bioinformatics* 28:2223–2230. DOI:
570 10.1093/bioinformatics/bts429.
- 571 Itävaara M, Nyssönen M, Kapanen A, Nousiainen A, Ahonen L, Kukkonen I. (2011).
572 Characterization of bacterial diversity to a depth of 1500 m in the Outokumpu deep
573 borehole, Fennoscandian Shield. *FEMS Microbiol Ecol* 77:295–309. DOI:
574 10.1111/j.1574-6941.2011.01111.x.
- 575 Jungbluth SP, Bowers R, Lin H-T, Cowen JP, Rappé MS. (2016). Novel microbial assemblages
576 inhabiting crustal fluids within mid-ocean ridge flank subsurface basalt. *ISME J* 10:2033–
577 2047. DOI: 10.1038/ismej.2015.248.
- 578 Jungbluth SP, Grote J, Lin H-T, Cowen JP, Rappé MS. (2013). Microbial diversity within
579 basement fluids of the sediment-buried Juan de Fuca Ridge flank. *ISME J* 7:161–172.
580 DOI: 10.1038/ismej.2012.73.

- 581 Jungbluth SP, Lin H-T, Cowen JP, Glazer BT, Rappé MS. (2014). Phylogenetic diversity of
582 microorganisms in subseafloor crustal fluids from Holes 1025C and 1026B along the
583 Juan de Fuca Ridge flank. *Front Microbiol* 5:119. DOI: 10.3389/fmicb.2014.00119.
- 584 Krzywinski M, Schein J, Birol I, Connors J, Gascoyne R, Horsman D, *et al.* (2009). Circos: an
585 information aesthetic for comparative genomics. *Genome Res* 19:1639–1645. DOI:
586 10.1101/gr.092759.109.
- 587 Labonté JM, Field EK, Lau M, Chivian D, van Heerden E, Wommack KE, *et al.* (2015). Single
588 cell genomics indicates horizontal gene transfer and viral infections in a deep subsurface
589 Firmicutes population. *Front Microbiol* 6:349. DOI: 10.3389/fmicb.2015.00349.
- 590 Langmead B, Salzberg SL. (2012). Fast gapped-read alignment with Bowtie 2. *Nat Methods*
591 9:357–359. DOI: 10.1038/nmeth.1923.
- 592 Lau MCY, Cameron C, Magnabosco C, Brown CT, Schilkey F, Grim S, *et al.* (2014). Phylogeny
593 and phylogeography of functional genes shared among seven terrestrial subsurface
594 metagenomes reveal N-cycling and microbial evolutionary relationships. *Front Microbiol*
595 5:531. DOI: 10.3389/fmicb.2014.00531.
- 596 Lerm S, Westphal A, Miethling-Graff R, Alawi M, Seibt A, Wolfgramm M, *et al.* (2013).
597 Thermal effects on microbial composition and microbiologically induced corrosion and
598 mineral precipitation affecting operation of a geothermal plant in a deep saline aquifer.
599 *Extremophiles* 17:311–327. DOI: 10.1007/s00792-013-0518-8.
- 600 Letunic, I, Bork, P (2016). Interactive tree of life (iTOL) v3: an online tool for the display and
601 annotation of phylogenetic and other trees, *Nucleic Acids Research* 44 (W1): W242-
602 W245. DOI: 10.1093/nar/gkw290.
- 603 Lin H-T, Cowen JP, Olson EJ, Amend JP, Lilley MD. (2012). Inorganic chemistry, gas
604 compositions and dissolved organic carbon in fluids from sedimented young basaltic
605 crust on the Juan de Fuca Ridge flanks. *Geochim Cosmochim Acta* 85:213–227. DOI:
606 10.1016/j.gca.2012.02.017.
- 607 Lin H-T, Cowen JP, Olson EJ, Lilley MD, Jungbluth SP, Wilson ST, *et al.* (2014). Dissolved
608 hydrogen and methane in the oceanic basaltic biosphere. *Earth Planet Sci Lett* 405:62–
609 73. DOI: 10.1016/j.epsl.2014.07.037.

- 610 Lin L-H, Wang P-L, Rumble D, Lippmann-Pipke J, Boice E, Pratt LM, *et al.* (2006). Long-term
611 sustainability of a high-energy, low-diversity crustal biome. *Science* 314:479–482. DOI:
612 10.1126/science.1127376.
- 613 Lowe TM, Eddy SR. (1997). tRNAscan-SE: a program for improved detection of transfer RNA
614 genes in genomic sequence. *Nucleic Acids Res* 25:955–964. DOI: 10.1093/nar/25.5.0955.
- 615 Loy A, Duller S, Baranyi C, Mussmann M, Ott J, Sharon I, *et al.* (2009). Reverse dissimilatory
616 sulfite reductase as phylogenetic marker for a subgroup of sulfur-oxidizing prokaryotes.
617 *Environ Microbiol* 11:289–299. DOI: 10.1111/j.1462-2920.2008.01760.x.
- 618 Ludwig W, Strunk O, Westram R, Richter L, Meier H, Yadhukumar, *et al.* (2004). ARB: a
619 software environment for sequence data. *Nucleic Acids Res* 32:1363–1371. DOI:
620 10.1093/nar/gkh293.
- 621 Lukashin AV, Borodovsky M. (1998). GeneMark.hmm: new solutions for gene finding. *Nucleic*
622 *Acids Res* 26:1107–1115. DOI: 10.1093/nar/26.4.1107.
- 623 Luo R, Liu B, Xie Y, Li Z, Huang W, Yuan J, *et al.* (2012). SOAPdenovo2: an empirically
624 improved memory-efficient short-read de novo assembler. *Gigascience* 1:18. DOI:
625 10.1186/2047-217X-1-18.
- 626 Magnabosco C, Tekere M, Lau MCY, Linage B, Kuloyo O, Erasmus M, *et al.* (2014).
627 Comparisons of the composition and biogeographic distribution of the bacterial
628 communities occupying South African thermal springs with those inhabiting deep
629 subsurface fracture water. *Front Microbiol* 5:679. DOI: 10.3389/fmicb.2014.00679.
- 630 Marchler-Bauer A, Anderson JB, DeWeese-Scott C, Fedorova ND, Geer LY, He S, *et al.* (2003).
631 CDD: a curated Entrez database of conserved domain alignments. *Nucleic Acids Res*
632 31:383–387. DOI: 10.1093/nar/gkg087.
- 633 Markowitz VM, Chen I-MA, Chu K, Szeto E, Palaniappan K, Pillay M, *et al.* (2014). IMG/M 4
634 version of the integrated metagenome comparative analysis system. *Nucleic Acids Res*
635 42:D568–73. DOI: 10.1093/nar/gkt919.
- 636 Markowitz VM, Chen I-MA, Palaniappan K, Chu K, Szeto E, Grechkin Y, *et al.* (2012). IMG:
637 the Integrated Microbial Genomes database and comparative analysis system. *Nucleic*
638 *Acids Res* 40:D115–22. DOI: 10.1093/nar/gkr1044.

- 639 Matsen FA, Kodner RB, Armbrust EV. (2010). pplacer: linear time maximum-likelihood and
640 Bayesian phylogenetic placement of sequences onto a fixed reference tree. *BMC*
641 *Bioinformatics* 11:538. DOI: 10.1186/1471-2105-11-538.
- 642 Miller CS, Baker BJ, Thomas BC, Singer SW, Banfield JF. (2011). EMIRGE: reconstruction of
643 full-length ribosomal genes from microbial community short read sequencing data.
644 *Genome Biol* 12:R44. DOI: 10.1186/gb-2011-12-5-r44.
- 645 Morgulis A, Gertz EM, Schäffer AA, Agarwala R. (2006). A fast and symmetric DUST
646 implementation to mask low-complexity DNA sequences. *J Comput Biol* 13:1028–1040.
647 DOI: 10.1089/cmb.2006.13.1028.
- 648 Niu B, Zhu Z, Fu L, Wu S, Li W. (2011). FR-HIT, a very fast program to recruit metagenomic
649 reads to homologous reference genomes. *Bioinformatics* 27:1704–1705. DOI:
650 10.1093/bioinformatics/btr252.
- 651 Noguchi H, Park J, Takagi T. (2006). MetaGene: prokaryotic gene finding from environmental
652 genome shotgun sequences. *Nucleic Acids Res* 34:5623–5630. DOI: 10.1093/nar/gkl723.
- 653 Parks DH, Imelfort M, Skennerton CT, Hugenholtz P, Tyson GW. (2015). CheckM: assessing
654 the quality of microbial genomes recovered from isolates, single cells, and metagenomes.
655 *Genome Res* 25:1043–1055. DOI: 10.1101/gr.186072.114.
- 656 Price, MN, Dehal, PS, Arkin, AP. (2010). FastTree 2- Approximately maximum-likelihood trees
657 for large alignments. *PLoS ONE* 5:e9490. DOI: 10.1371/journal.pone.0009490.
- 658 Pruesse E, Peplies J, Glöckner FO. (2012). SINA: accurate high-throughput multiple sequence
659 alignment of ribosomal RNA genes. *Bioinformatics* 28:1823–1829. DOI:
660 10.1093/bioinformatics/bts252.
- 661 R Core Team. (2015). R: A Language and Environment for Statistical Computing. Vienna,
662 Austria. ISBN: 3-900051-07-0.
- 663 Rho M, Tang H, Ye Y. (2010). FragGeneScan: predicting genes in short and error-prone reads.
664 *Nucleic Acids Res* 38:e191. DOI: 10.1093/nar/gkq747.
- 665 Robador A, Jungbluth SP, LaRowe DE, Bowers RM, Rappé MS, Amend JP, *et al.* (2015).
666 Activity and phylogenetic diversity of sulfate-reducing microorganisms in low-
667 temperature subsurface fluids within the upper oceanic crust. *Front Microbiol* 5:748.
668 DOI: 10.3389/fmicb.2014.00748.

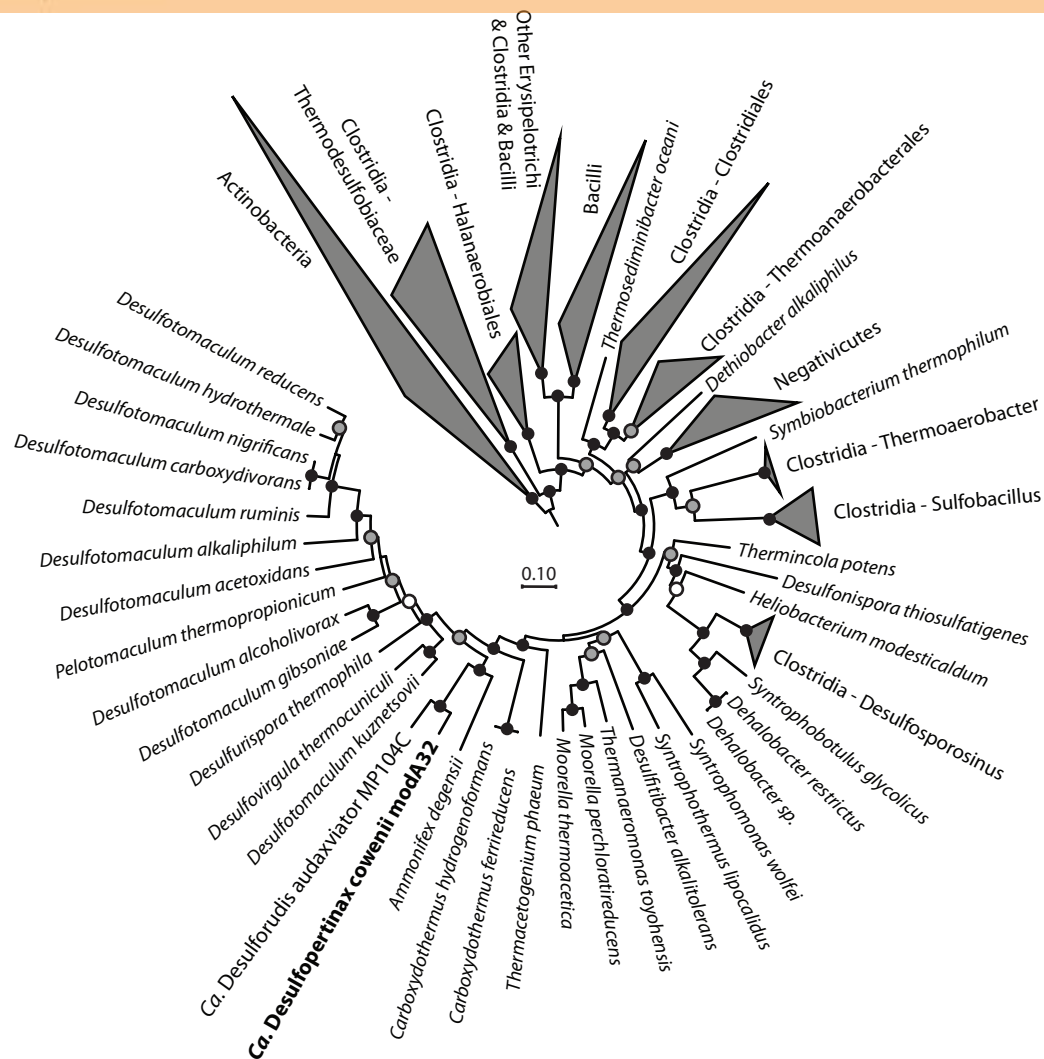
- 669 Stamatakis A. (2006). RAxML-VI-HPC: maximum likelihood-based phylogenetic analyses with
670 thousands of taxa and mixed models. *Bioinformatics* 22:2688–2690. DOI:
671 10.1093/bioinformatics/btl446.
- 672 Stamatakis A, Hoover P, Rougemont J. (2008). A rapid bootstrap algorithm for the RAxML Web
673 servers. *Syst Biol* 57:758–771. DOI: 10.1080/10635150802429642.
- 674 Sullivan MJ, Petty NK, Beatson SA. (2011). Easyfig: a genome comparison visualizer.
675 *Bioinformatics* 27:1009–1010. DOI: 10.1093/bioinformatics/btr039.
- 676 Tennessen K, Andersen E, Clingenpeel S, Rinke C, Lundberg DS, Han J, *et al.* (2016). ProDeGe:
677 a computational protocol for fully automated decontamination of genomes. *ISME J*
678 10:269–272. DOI: 10.1038/ismej.2015.100.
- 679 Tiago I, Verissimo A. (2013). Microbial and functional diversity of a subterrestrial high pH
680 groundwater associated to serpentinization. *Environ Microbiol* 15:1687–1706. DOI:
681 10.1111/1462-2920.12034.
- 682 Treangen TJ, Sommer DD, Angly FE, Koren S, Pop M. (2011). Next generation sequence
683 assembly with AMOS. *Curr Protoc Bioinformatics* Chapter 11:11.8. DOI:
684 10.1002/0471250953.bi1108s33.
- 685 Wheat CG, Jannasch HW, Kastner M, Hulme S, Cowen J, Edwards KJ, *et al.* (2011). Fluid
686 sampling from oceanic borehole observatories: design and methods for CORK activities
687 (1990-2010). *In* Proceedings of the Integrated Ocean Drilling Program Vol. 327 (eds. A.
688 T. Fisher, T. Tsuji, K. Petronotis, & Expedition 327 Scientists) 1-36 (Integrated Ocean
689 Drilling Program Management International, Inc., 2011). DOI:
690 10.2204/iodp.proc.327.109.2011.
- 691 Wu D, Jospin G, Eisen JA. (2013). Systematic identification of gene families for use as
692 “markers” for phylogenetic and phylogeny-driven ecological studies of bacteria and
693 archaea and their major subgroups. *PLoS ONE* 8:e77033. DOI:
694 10.1371/journal.pone.0077033.
- 695 Wu Y-W, Tang Y-H, Tringe SG, Simmons BA, Singer SW. (2014). MaxBin: an automated
696 binning method to recover individual genomes from metagenomes using an expectation-
697 maximization algorithm. *Microbiome* 2:26. DOI: 10.1186/2049-2618-2-26.

Figure 1(on next page)

Phylogenomic and shared gene content analysis of “*Ca. Desulfopertinax cowenii*”, “*Ca. Desulforudis audaxviator*” and other Firmicutes.

Analysis of phylogenomic relationships, percent shared genes, and average amino-acid identity between “*Ca. Desulfopertinax cowenii*” modA32 and “*Ca. Desulforudis audaxviator*” MP104C reveal two lineages similar to each other and distinct from other *Firmicutes*. (A) Phylogenomic relationships between “*Ca. D. cowenii*”, “*Ca. D. audaxviator*”, and other *Firmicutes* based on a concatenated amino acid alignment. Black (100%), gray (>80%), and white (>50%) circles indicate nodes with high local support values, from 1000 replicates. Actinobacteria (n=687) were used as an outgroup. The scale bar corresponds to 0.10 substitutions per amino acid position. (B) Percent shared genes (upper right) and average amino-acid identity (lower left) between “*Ca. D. cowenii*”, “*Ca. D. audaxviator*”, and six closely related *Firmicutes* lineages from panel (A). The grey scale distinguishing horizontal axis labels corresponds to genome size.

a



b

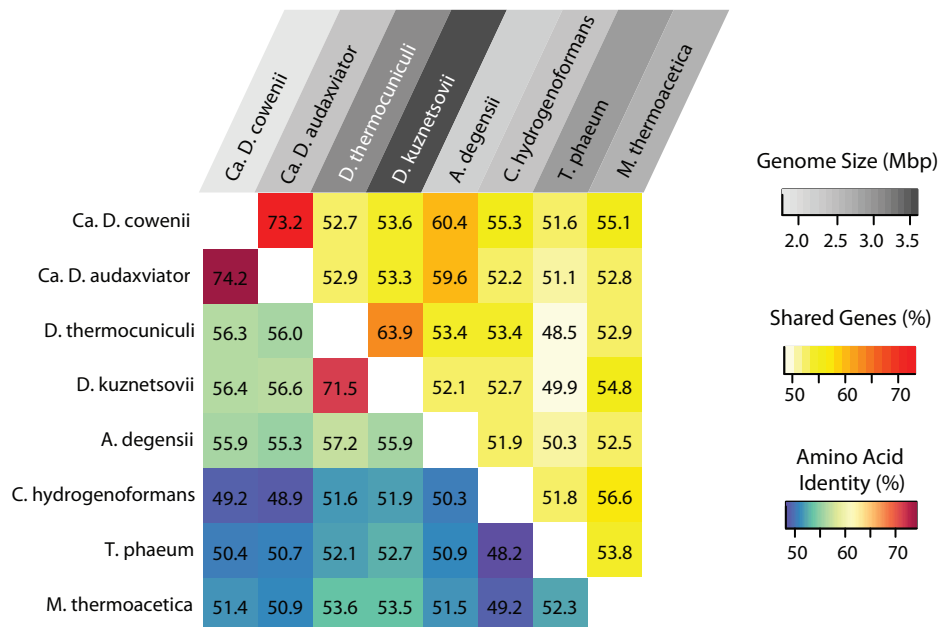
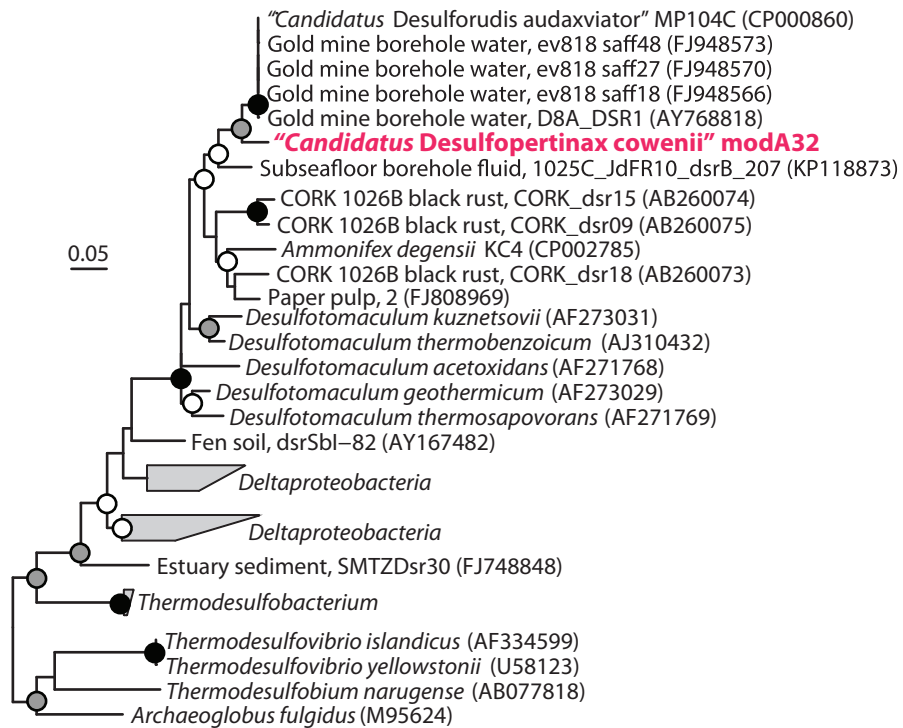


Figure 2 (on next page)

Phylogenetic analysis of “*Ca. Desulfopertinax cowenii*”, “*Ca. Desulforudis audaxviator*” and other closely related *dsrB* and SSU rRNA genes.

Phylogenetic relationships between “*Ca. Desulfopertinax cowenii*”, “*Ca. Desulforudis audaxviator*”, and closely related *dsrB* genes (A) and a SSU rRNA gene related to “*Ca. D. audaxviator*” reconstructed from the U1362A metagenome via EMIRGE (B) lend additional support to a shared evolutionary history between “*Ca. D. cowenii*” and “*Ca. D. audaxviator*”. Black (100%), gray ($\geq 80\%$), and white ($\geq 50\%$) circles indicate nodes with bootstrap support, from 2000 replicates. The scale bars correspond to 0.05 substitutions per nucleotide position.

a. *dsrB*

b. SSU rRNA

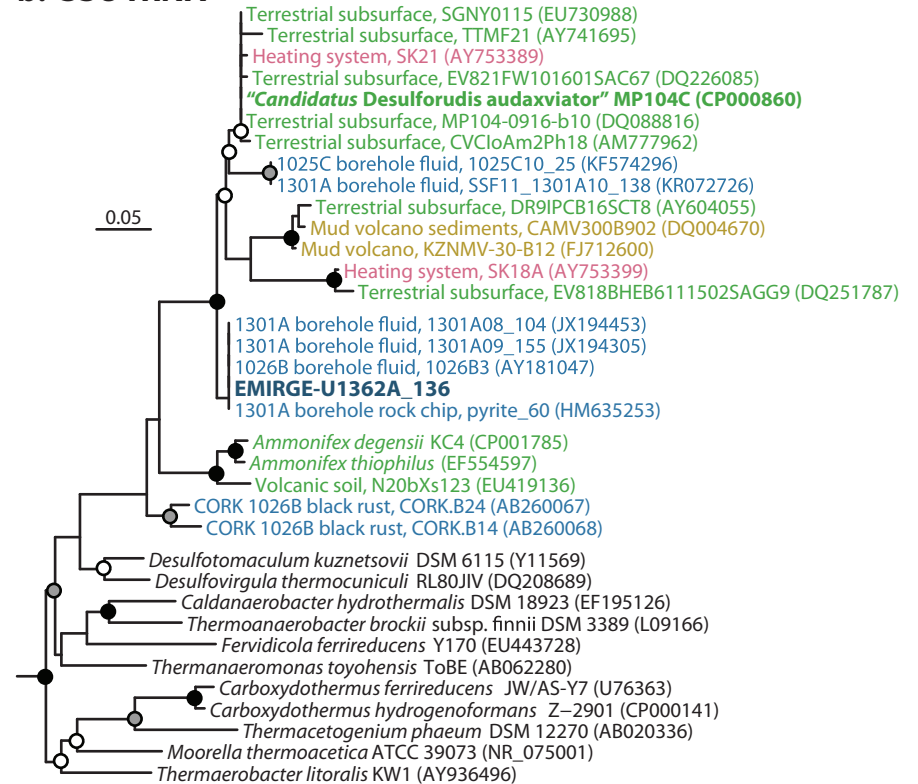


Figure 3(on next page)

Analysis of genome alignment and shared and unique gene inventories in “*Ca. Desulfopertinax cowenii*” and “*Ca. Desulforudis audaxviator*”.

Multiple genome alignment and analysis of shared and unique gene inventories reveal key conserved and variable features of “*Ca. Desulfopertinax cowenii*” and “*Ca. Desulforudis audaxviator*”. (A) Comparison of the “*Ca. D. cowenii*” genome scaffolds with “*Ca. D. audaxviator*” based on reciprocal best BLAST. From innermost to outermost, concentric circles show: nucleotide positions of genomes and scaffolds, percent GC content using a 100 bp sliding window, similarity of mapped U1362A reads. Links connecting circles are colored according to “*Ca. D. cowenii*” scaffold origin [Ga007115_(11-16)] and the degree of shading represents similarities (minimum similarity 70%) based on BLAST comparisons using < 75% (light shade), $\geq 75\%$ (dark shade) nucleic acid identity thresholds. (B) Frequency of reciprocal best BLAST hits (n=1364) by percent similarity. Percent similarity histogram bins are in 2% increments and the dashed lines indicate average nucleotide identity (red) and average amino acid identity (blue) between “*Ca. D. cowenii*” and “*Ca. D. audaxviator*”. Relative abundance of shared (C) and unique (D) genes in the “*Ca. D. cowenii*” and “*Ca. D. audaxviator*” genomes, sorted by annotated COG categories.

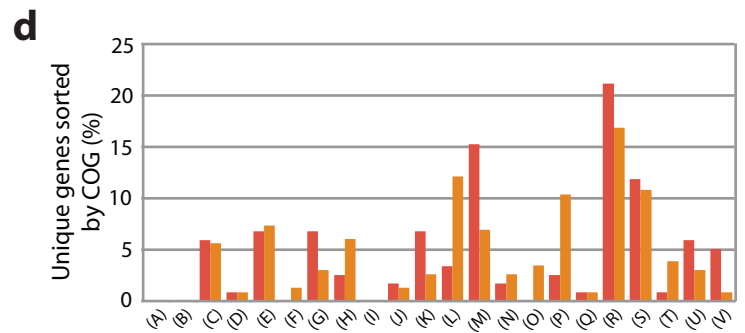
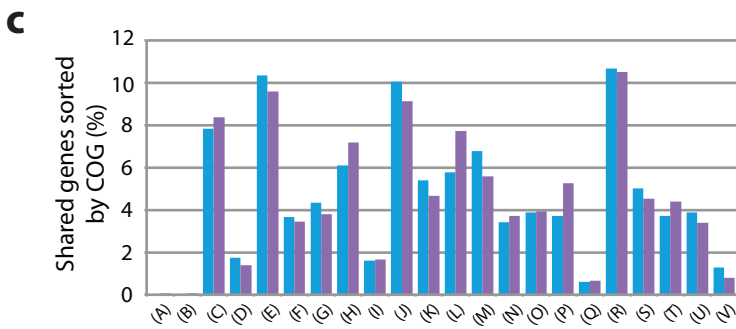
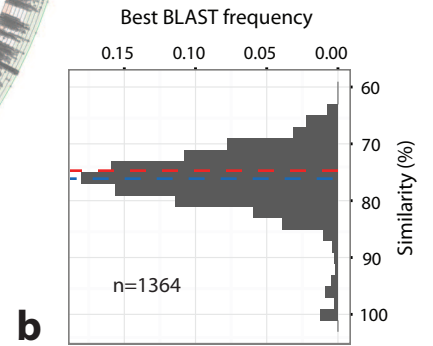
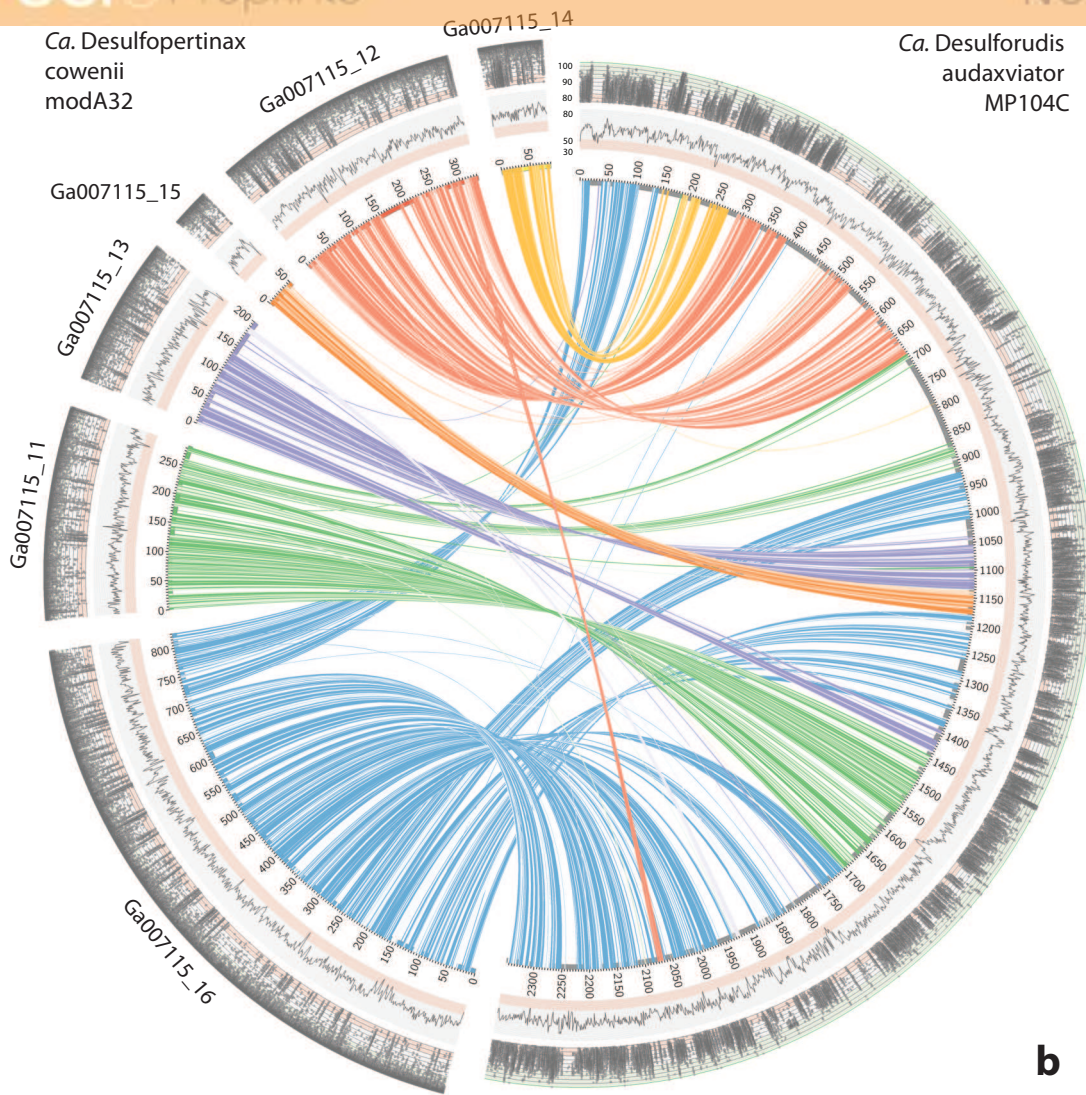


Figure 4(on next page)

Survey of Firmicutes genome characteristics.

Survey of *Firmicutes* genome size, genome GC content, and coding density separated by different classes (*Bacilli*, *Clostridia*, *Erysipelotrichi*, *Negativicutes*). Only complete genomes and genomes with GC content >20% were used (n=909). The genome size of “*Ca. Desulfopertinax cowenii*” was estimated by assuming the current genome length (1.78 Mbp) was 98% the total genome length. Classes are distinguished by shape, while genome size is indicated by shape size and color. All genomes were downloaded from IMG on December 13, 2015.

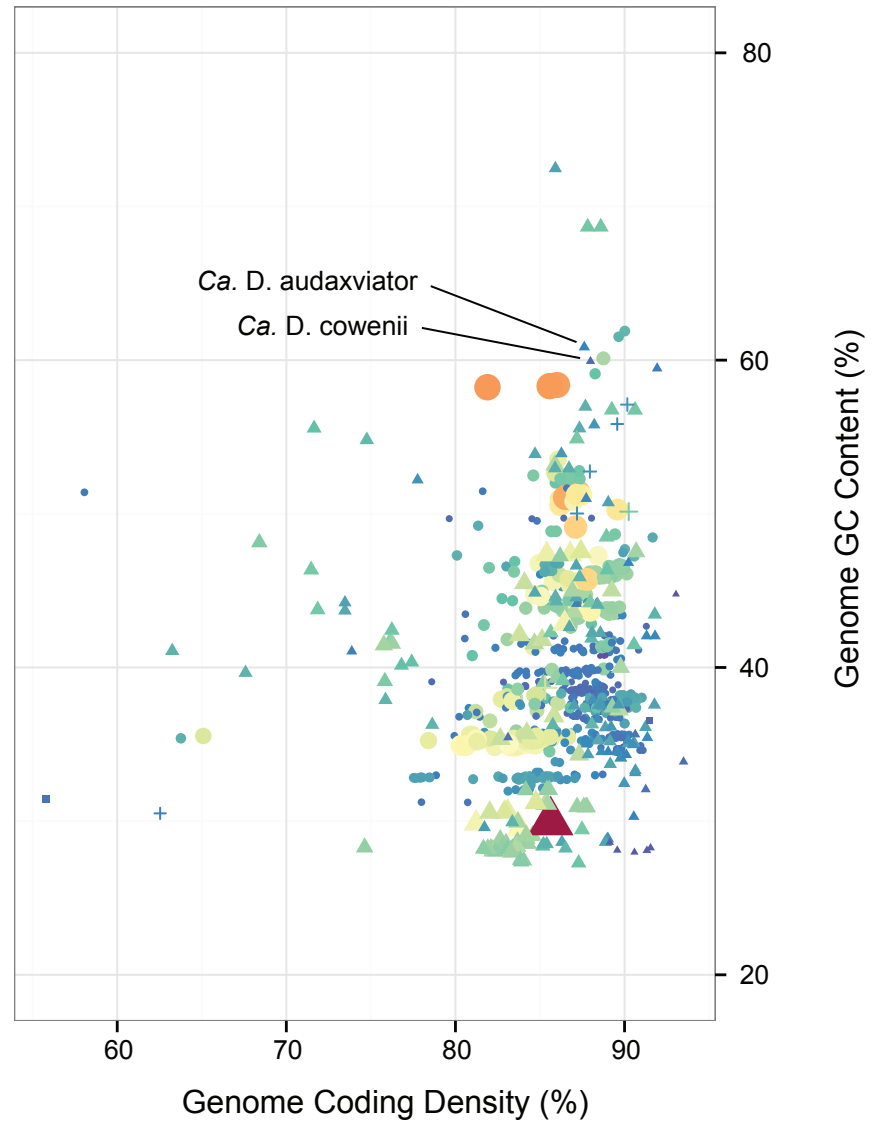
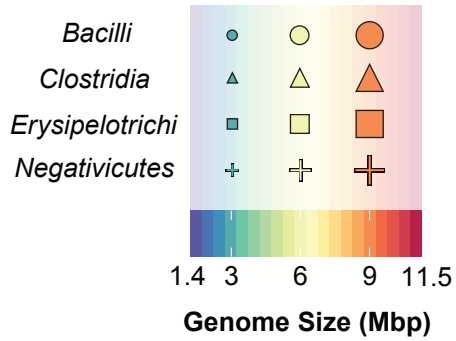
**Class
Firmicutes**

Figure 5(on next page)

Analysis of genome alignment between “*Ca. Desulfopertinax cowenii*”, “*Ca. Desulforudis audaxviator*” and five closely related single-cell genomes.

Comparison of terrestrial deep subsurface SAGs AC-310-P15, O10, N13, E02, and A06 with the genomes of “*Ca. Desulfopertinax cowenii*” and “*Ca. Desulforudis audaxviator*”. Links connecting colored circles represent similarities based on blastn comparisons allowing a maximum of two best hit and using 75 - 80% (green), 80 - 85% (blue), > 85% (grey) nucleic acid identity thresholds. Inset plot indicates blastn comparisons allowing a maximum of a two best hits.

Ca. Desulfopertinax
cowenii
modA32

Ca. Desulforudis
audaxviator
MP104C

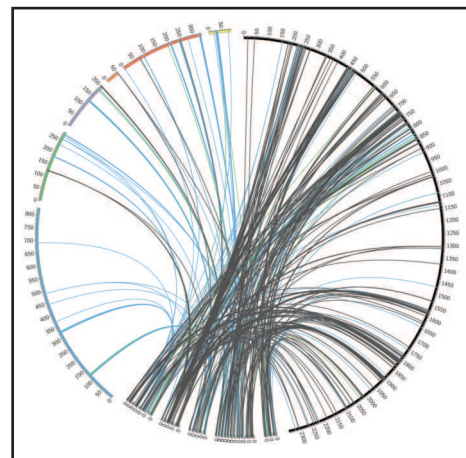
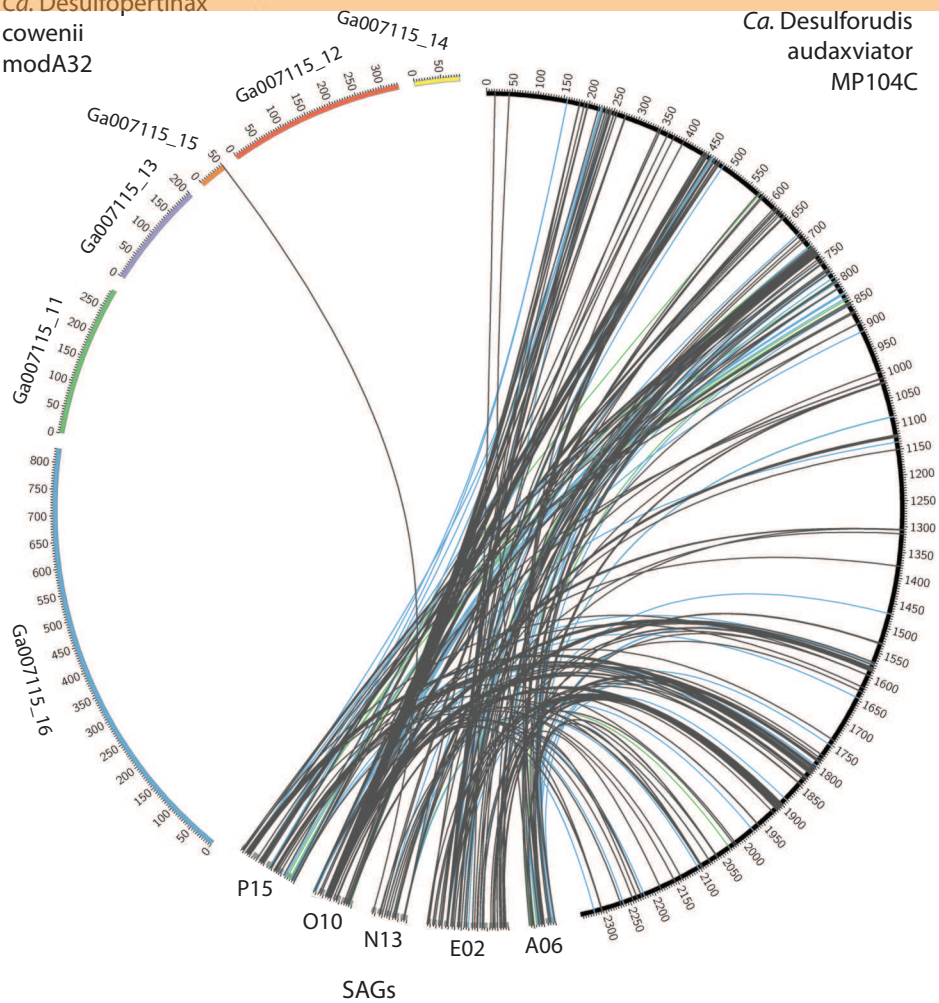


Figure 6(on next page)

Comparative analysis of genomic organization in “*Ca. Desulfopertinax cowenii*” and “*Ca. Desulforudis audaxviator*”.

Comparison of genomic organization in “*Ca. Desulfopertinax cowenii*” with “*Ca. Desulforudis audaxviator*” highlighting regions with large, internal insertion/deletion events containing no homologous genes in the opposing genome. (A) nitrogen-fixation operon, (B) vitamin B12 synthesis, (C) gas vesicle production, (D) a CRISPR-CAS array. Genes are colored according to COG categories and BLAST similarity between regions is indicated by shading intensity.

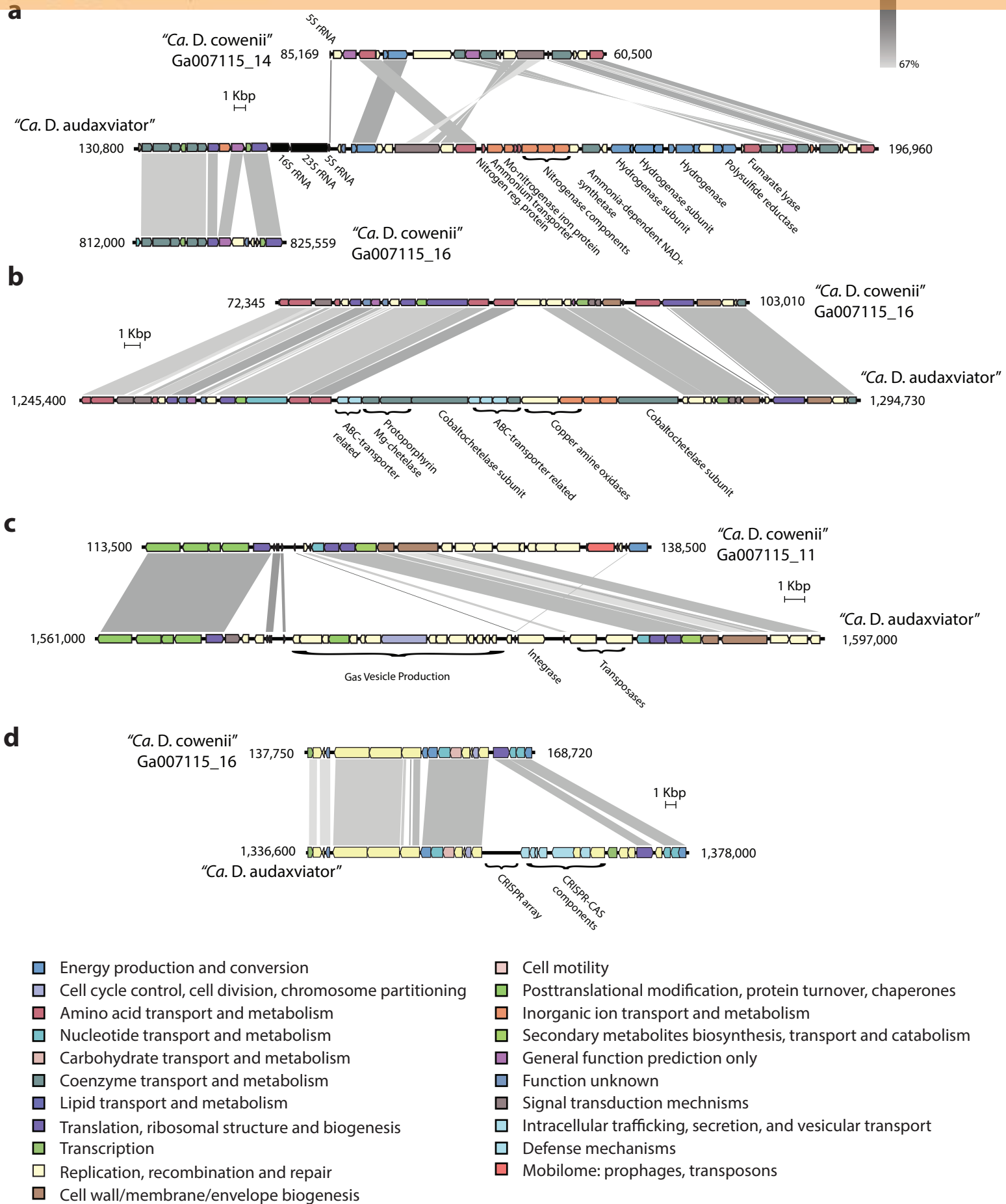


Figure 7 (on next page)

Analysis of the global distribution of "*Ca. Desulfopertinax cowenii*" and "*Ca. Desulforudis audaxviator*".

"*Ca. Desulfopertinax cowenii*" and "*Ca. Desulforudis audaxviator*" are globally-distributed in the deep subsurface. (A) Ellipse sizes correspond to the frequency of mapped reads from environmental metagenomes to "*Ca. D. cowenii*" and "*Ca. D. audaxviator*" genomes. Triangles indicate locations where a lineage has been detected in SSU rRNA gene surveys. The average frequency of reads mapped to "*Ca. D. cowenii*" and "*Ca. D. audaxviator*" are shown for all metagenomes listed in Supplementary Table 2 with >50000 genes. (B) Graphical representation of the frequency of environmental genome reads mapping to the "*Ca. D. cowenii*" and "*Ca. D. audaxviator*" genomes using a 96% read similarity score. Environmental metagenomes with the highest ratio of reads mapped to "*Ca. D. cowenii*" vs. "*Ca. D. audaxviator*" and having an average frequency of ≥ 0.00025 mapped reads are ordered in clockwise fashion from highest to lowest (Supplementary Table 2). MG-RAST metagenome 4440282 was retained solely because it had the highest ratio of reads mapped to "*Ca. D. cowenii*": "*Ca. D. audaxviator*". Links are colored according to the environmental source of each metagenome, while link sizes are proportional to the frequency of a read from a metagenome to map to one genome or the other. The log of metagenome size (number of reads) was used to create the relative length of the outer edges of the circle, which coarsely divide the environments into marine versus terrestrial. The "*Ca. D. cowenii*" genome is sized 2.2x the largest displayed metagenome and "*Ca. D. audaxviator*" is 1.32x (ratio of genome sizes) larger than the "*Ca. D. cowenii*" genome.

b

NOT PEER-REVIEWED

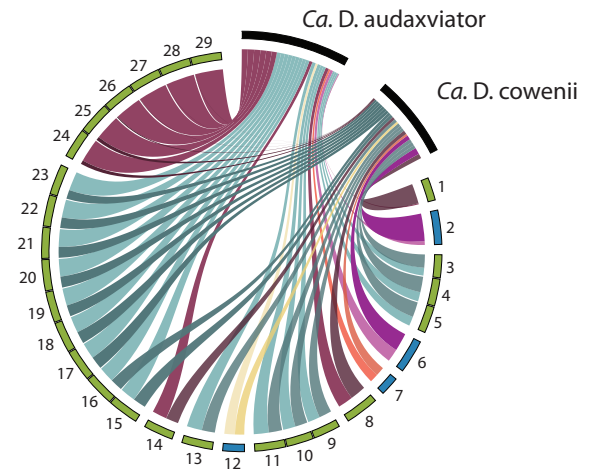
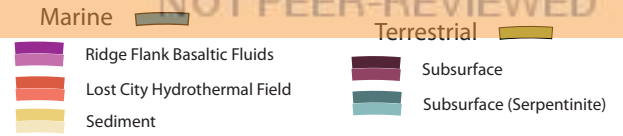
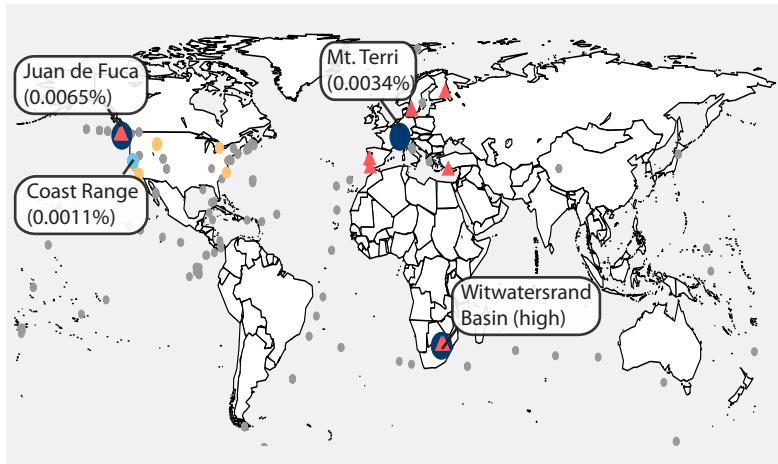


Table 1 (on next page)

Genome characteristics of “*Ca. Desulfopertinax cowenii*” modA32 and “*Ca. Desulforudis audaxviator*” MP104C.

1

	<i>“Ca. D. cowenii”</i>	<i>“Ca. D. audaxviator”</i>
Percent complete	98-99% (6 scaffolds)	100% (closed)
Genome size (bp)	1,778,734	2,349,476
Percent coding	89.8%	87.6%
GC content	60.2%	60.9%
Total no. of genes	1842	2293
No. of protein coding genes	1782 (96.7%)	2239 (97.6%)
With function prediction	1518 (85.2%)	1587 (70.9%)
Without function prediction	264 (14.8%)	652 (29.1%)
Shared	1514 (85.0%)	1606 (71.7%)
Paralogs	137	265
Pseudogenes	n.d. ^a	82
rRNA genes	2	6
5S rRNA	2	2
16S rRNA	n.d.	2
23S rRNA	n.d.	2
tRNA genes	44	45
CRISPR elements	1	4
Mobile elements (integrases/transposons)	6/7	23/81

2 ^an.d. – not detected

3

Table 2 (on next page)

“*Ca. Desulforudis audaxviator*” MP104C-related genome bins from the U1362A metagenome, analyzed by CheckM.

1

Bin_ID	Total contigs/ N50 (Kbp)/ longest contig (Kbp)	Completeness (%)	Contamination (%)	Strain Heterogeneity (%)	Total Bases (Mbp)
D. audaxviator	--	98.09	0.32	0	2.35
1362A_maxbin32	50/112/179	97.61	5.10	100	1.87
1362A_maxbin32 (ProDeGe filtered)	31/112/179	95.70	5.10	100	1.81
“ <i>Ca. D. cowenii</i> ” modA32 (SPAdes reassembly, ProDeGe filtered)	6/332/826	97.61	0	0	1.78

2